

**PROPERTIES OF NUCLEAR MATTER AND THE FRAGMENTS
FORMATION ON RELATIVISTIC BEAMS
OF THE NUCLOTRON/NICA COMPLEX.**

(in the framework of topic 02-1-1087-2009/2020)

FASA Project

FTE 6.3

*S.P. Avdeyev¹, H.Yu. Abramyan¹, A.S. Botvina², W. Karcz¹, V.V. Kirakosyan³,
L.V. Karnushina¹, E.M. Kozulin³, A.G. Litvinenko¹, E. Norbeck⁴,
V.F. Peresedov¹, P.A. Rukoyatkin¹, V.I. Stegaylov⁵, O.V. Strelakovsky³*

¹JINR, LHEP, Dubna, Russia

²Frankfurt Institute for Advanced Studies, Frankfurt am Main, Germany

³JINR, LNR, Dubna, Russia

⁴University of Iowa, Iowa City, USA

⁵JINR, LNP, Dubna, Russia

Project leader:

Doctor of Physical and Mathematical Sciences S.P. Avdeyev

Deputy of project leader:

Doctor of Physical and Mathematical Sciences A.G. Litvinenko

INTRODUCTION

The process of multiple fragment emission is the main decay mode of hot nuclei at excitation energies exceeding 3 MeV per nucleon. Hot nucleus, expanding under thermal pressure, falls into the spinodal region, which is limited by equal to zero nuclear rigidity: $\partial p/\partial V=0$ (Fig. 1). It is followed by copious emission of intermediate mass fragments (IMF), which are heavier than alpha particles but lighter than fission fragments. The experimental information about the spinodal state of nuclear matter is gained by studies of nuclear multifragmentation. The process is interpreted as a “liquid-gas” phase transition occurring at a temperature 5-7 MeV. The process has been intensively studied in recent years in nuclear-nuclear collisions [1-3].

The reaction mechanism is composed of three steps. The first step is the energy deposition step, when energetic nucleons and pions are emitted and the nuclear remnant is excited. This step is considered using the intranuclear cascade model (INC). We use the Dubna version of the INC [4] to get the distribution of the nuclear remnants in charge, mass, and excitation energy. The second step is expansion driven by the thermal pressure in the hot remnant, which is described in the spirit of the Expanding Emitting Source model, EES [5]. This process results in reducing the excitation energy. The final stage we describe by using the Statistical Model of Multifragmentation (SMM) [6]. Within this model the probabilities of different decay channels of the excited remnant are proportional to their statistical weights. The volume of the system from which emission of fragments occurs determines the Coulomb energy of the system.

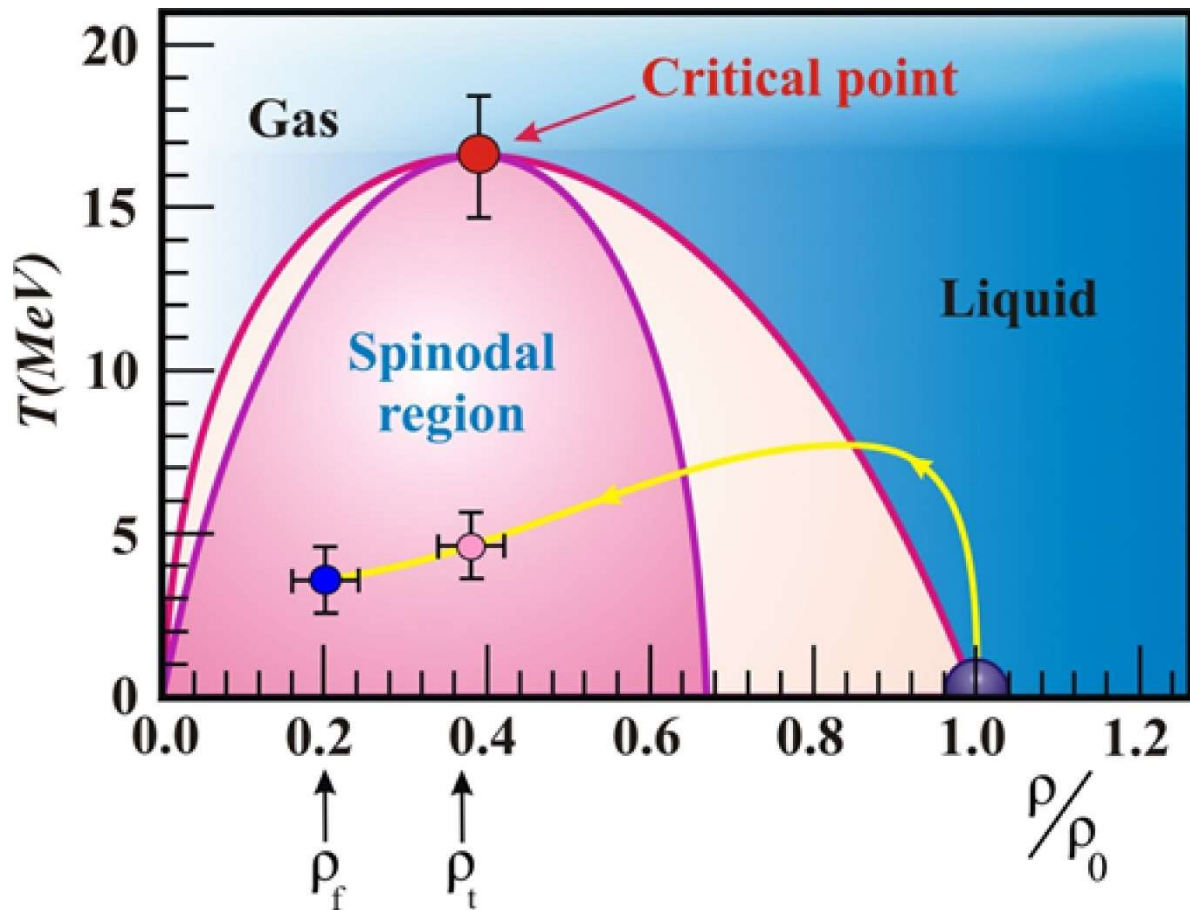


Fig.1. The spinodal region for the nuclear system. Temperature and baryon density are shown on the axes. Yellow line shows the way of the system from the starting point at $T = 0$ to the ρ_t , where prefragments are formed, and multiscission point at ρ_f .

Experiments on the relativistic beams of the Nuclotron accelerator using 4π -FASA device will provide information on the spinodal state of nuclear matter. The relevance of research is doubtless, because we are talking about the experimental study of nuclei with extreme excitation energy (comparable to the total binding energy of the nucleus). The Project will answer key questions about the time scale of fragment emission (there is a sequential emission of fragments or simultaneous breakup of the system), about degree of thermalization of the system before the breakup, and about radial flow.

The project is based on a huge methodological experience of the team gained in the research of nuclear multifragmentation in relativistic light ions beams in the last decade.

JUSTIFICATION

The aim of the Project is to study the properties of hot nuclei (with excitation energy more than 3 MeV per nucleon) produced in collisions of light relativistic ions with heavy targets. Hot nucleus, expanding due to thermal pressure, falls into the region of phase instability (spinodal region). As a result of density fluctuations, a homogeneous nuclear system disintegrates into an ensemble consisting of fragments and nucleons. The main goal is *the study of the space-time characteristics of hot nuclei and collective flows* formed in these interactions.

Experimental procedure based on the 4π -device FASA [7,8], including 30 dE-E telescopes for the detection of charged particles. Each telescope (TS) consists of a cylindrical ionization chamber (dE) and Si(Au) detectors to measure the total energy of the fragment. TS allow identify the charge of the fragments and determine its kinetic energy. Figure 2 shows device with a set of telescopes in the foreground. Target (gold film thickness of 1.5 mg/cm^2) is located in the center of the vacuum chamber.

The main part of the total solid angle of the device detector is the fragments multiplicity detector (FMD) which consists of 58 CsI(Tl) scintillators (25 mg/cm^2 thickness). FMD allow register fragments with $Z_f \geq 2$, determine their multiplicity, and their space distribution. Multiplicity selection allows you to “change” the average excitation energy of the fragmenting nucleus. In addition, the detector gives spatial picture of fragments in the event. Besides, measurement of fragments correlation is possible (TS-TS or TS-FMD). In this way, information on the time scale of the multifragmentation can be obtained. This is due to the fact that the shape of the correlation function is determined by the size and lifetime of the source. Figure 3 shows the inside of the device. It's a polyhedron that consists of 12 regular pentagons, surrounded by 60 irregular hexagons. This polyhedron can be made from the Archimedean pentagonal hexecontahedron, consisting of 60 irregular pentagons, by cutting 12 pentagonal vertices. The cut-off line is chosen to make the solid angles of all detectors equal. The general view of FASA setup is shown in Figure 4. The main body of the device is a welded steel frame with the shape of a dodecahedron, ten sides of which carry steel flanges with six counters. Two flanges centered on the beam axis are connected with the entry and exit pipes of 200 mm diameter. These flanges have only five counters. The entry and exit pipes rest of semicircular supports fixed at the top of steel pillars. The device can be rotated around the horizontal axis and fixed as necessary for comfortable mounting. Vacuum gas distributor mounted on the platform.

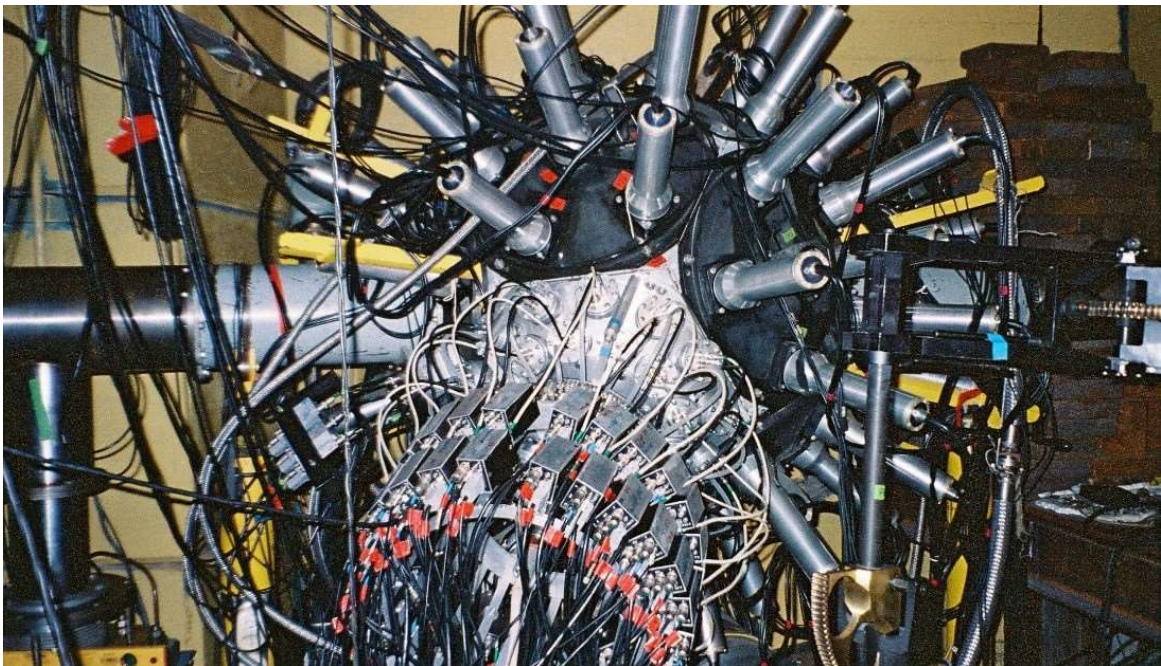


Fig. 2. FASA device on the Nuclotron beam. Electronics of dE-E telescopes in the foreground. Aluminum cylinders – the multiplicity detectors of fragments.

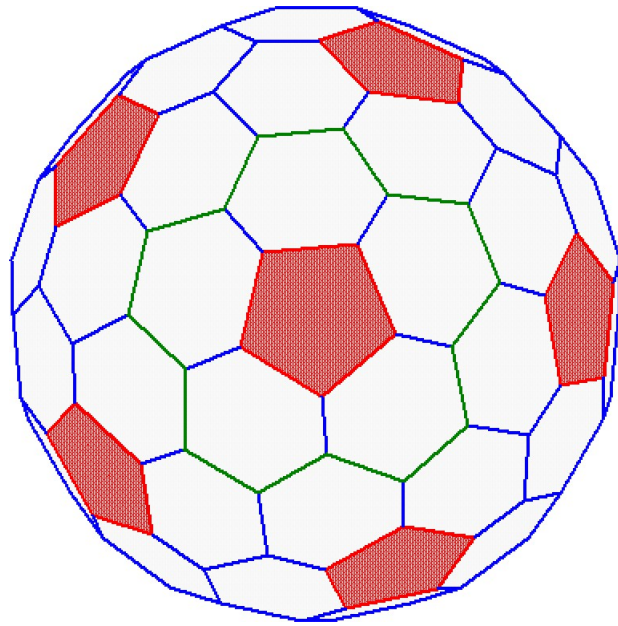


Fig. 3. The polyhedron formed by the front faces of the CsI(Tl) detectors. The pentagons are marked in red, the irregular hexagons in white

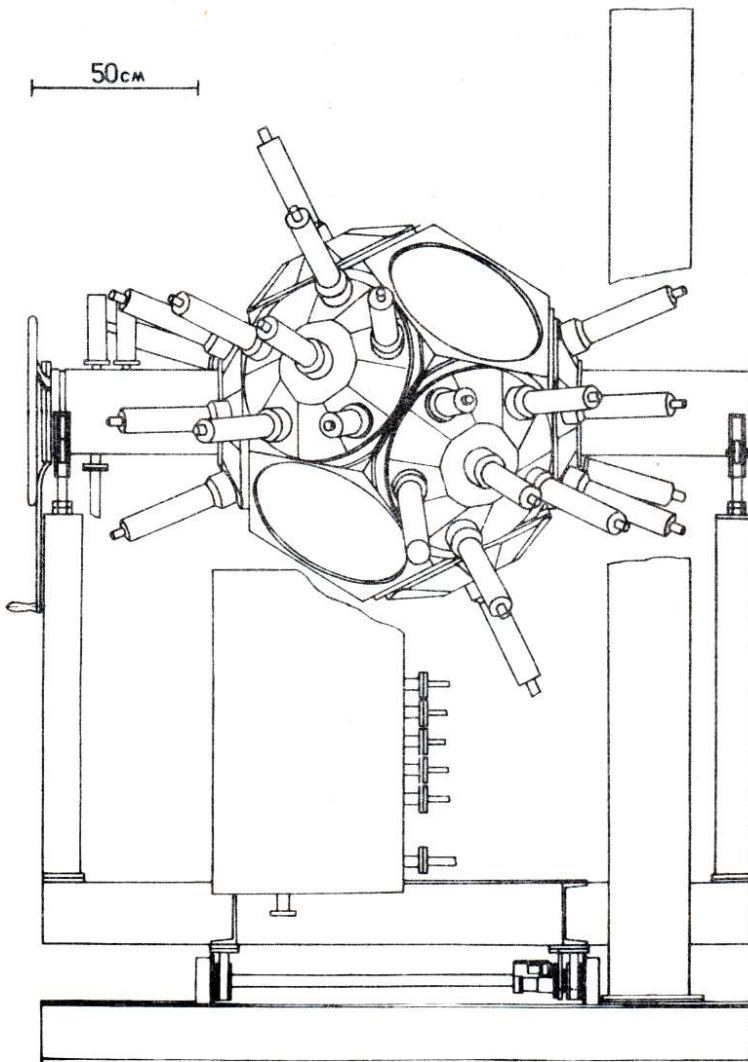


Fig. 4. General view of FASA device.

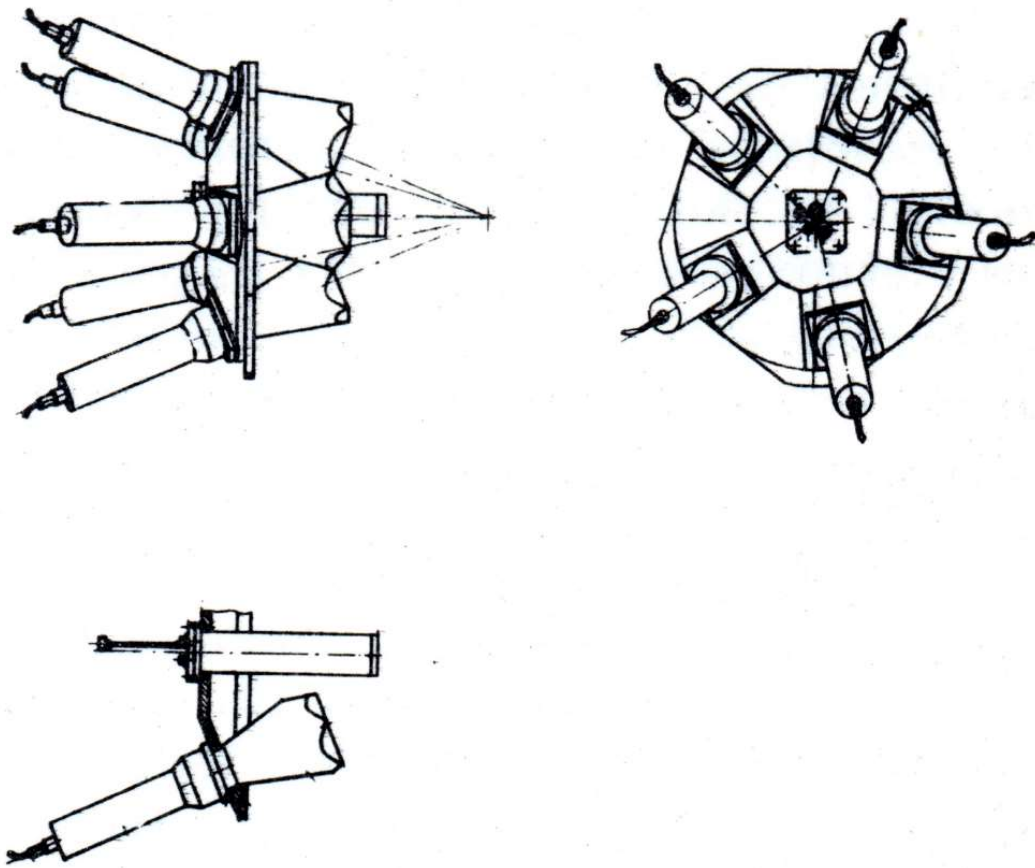


Fig. 5. One of the modules of FASA device consisting of five CsI(Tl) scintillators and device to enter the target and the calibration source.

Figure 5 shows one module with five scintillation counters. The central counter is replaced by a device that allows to enter a thin target ($\sim 1.5 \text{ mg/cm}^2$) or α -source into the center of the camera (using electromechanical drive). Scintillation counters have a specially shaped light guide: hexagon or pentagon on the side of the scintillator goes into the cylinder on the side of the photomultiplier. Light guide length 20 cm, diagonal scintillator size $\approx 15 \text{ cm}$. Distance from target center to scintillator center $\sim 30 \text{ cm}$. Photomultipliers FEU-110 are used, having the most adequate photocathode for CsI(Tl). Scintillators are made in the form of thin polycrystalline film on a plexiglass backing by vacuum thermal spraying [9]. Figure 6 shows the calculated dependences of the amplitude of the light flash as a function of the energy of various particles for a scintillator with a thickness of 25 mg/cm^2 . Calculations are performed using data from work [10]. It can be seen that there is a satisfactory separation in amplitude of α -particles with energy up to 60 MeV from protons. For heavier fragments the situation is more favorable (bring in mind that the main intensity in the spectrum of intermediate mass fragments with $Z_f = 3 - 15$ is in the energy range 10-80 MeV).

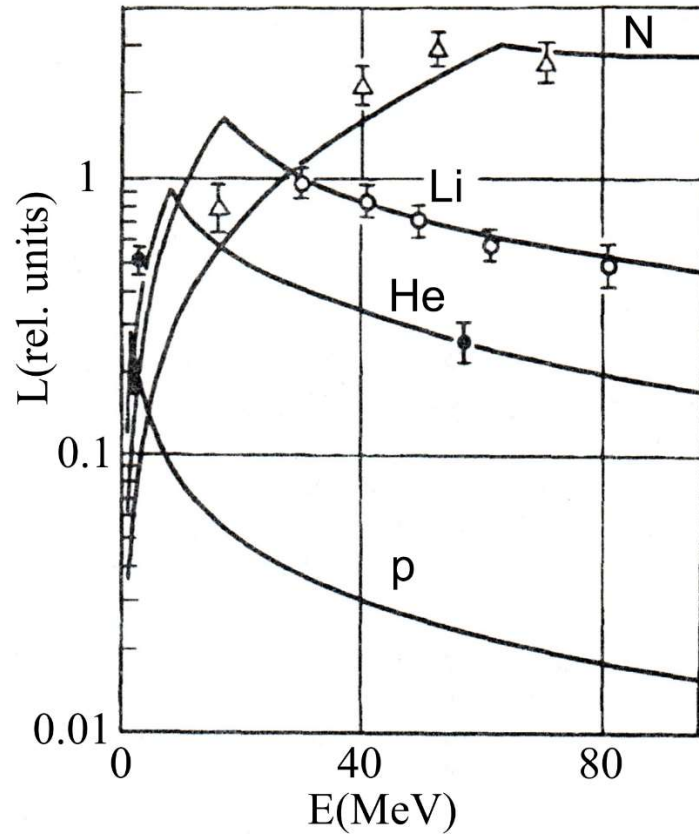


Fig. 6. The amplitude of the flash in a CsI(Tl) layer 25 mg/cm^2 thick versus the energy of different particles. The flash amplitude that is detected when an 8.78 MeV α -particle is absorbed completely is taken as the unit along the ordinate axis. The solid lines are calculated, the points are experimental.

Device includes 30 TS. 5 telescopes are located at the following angles to the beam direction: 24° , 68° , 87° , 112° , 156° . 25 telescopes assembled in a compact design on the flange (Fig. 7) with polar angles $37^\circ < \Theta < 87^\circ$. Each telescope consists of an ionization chamber (dE) and Si(Au)-detector. The casing of the telescope detectors is made of duralumin in the shape of the truncated cone with a length of 83 mm and diameters of 64 and 54 mm. The entrance window is made of a $1.5 \mu\text{m}$ thick Mylar film, which is attached to the brass grid with a thickness of 2 mm and transparency of 74%. The ionization chamber has a cylindrical shape with an active region 30 mm in diameter and 35 mm long. The brass cathode is grounded, and the anode is a 0.5 mm diameter gold wire, which is fixed in place in glass tubes with a 3 mm diameter and 1 mm thick walls. The voltage of 600 V is applied to the anode via a metal wire enclosed in one of these tubes. To reduce the edge effect, the other end of the anode wire is sealed in the glass tube, and films with a deposited gold coating are placed on both sides of the chamber and are grounded. The working volume is filled with CF_4 at a pressure of 50 Torr. The design of the ionization chamber ensures charge collection across particle tracks. This helps reduce the probability of recombination in nuclear fragment detection. Residual energy E of particles is determined by the semiconductor Si detector with an operating diameter of 40 mm and a thickness of $750 \mu\text{m}$, which is sufficient for full stopping of fragments with $Z > 3$ (some high energy α particles and Li nuclei shoot through the detector, losing only part of their energy). The detector casing is fixed in place behind the ionization chamber.

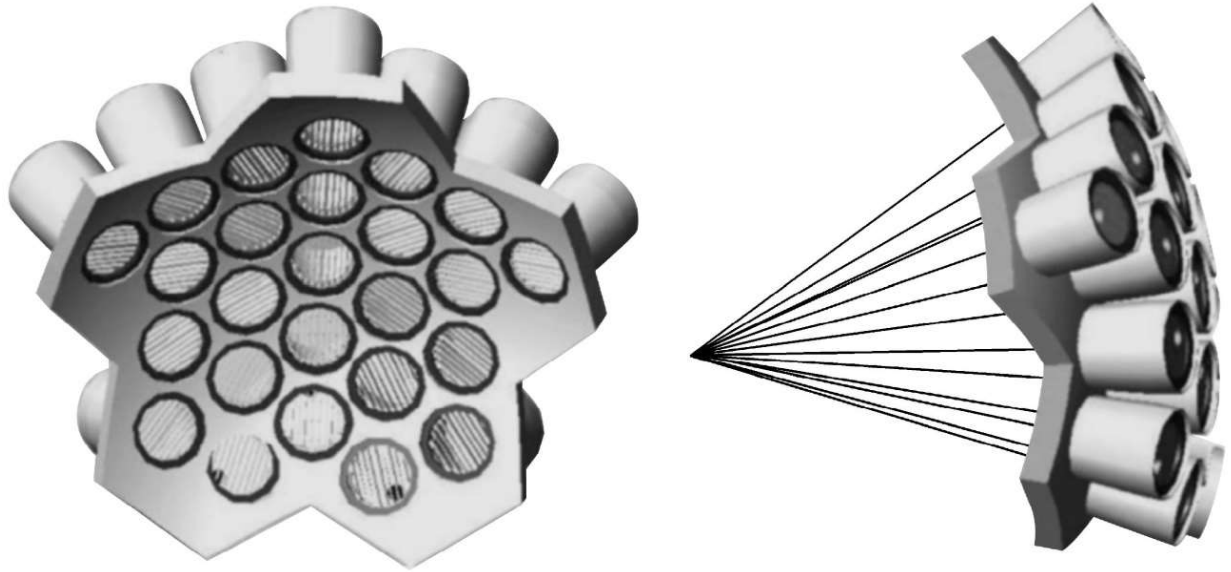


Fig. 7. General view of the detector module composed of 25 telescopespectrometers.

An α source (^{241}Am) for energy calibration is glued on the detector surface. Pulses in the ionization chamber are formed for a longer time than in the semiconductor detector. The use of 5 + 25 telescopes allows for correlation measurements at relative angles in the range from 10° to 180° . At the same time, the charges and energies of both fragments are fixed.

Figure 8 shows a block diagram for converting analog signals into a digital sequence implemented in the VME standard and then recorded in a computer. There is multi-event buffer - dual port memory which can store up to 32 events. Number of signals to be digitized 176 (30 dE ; 30 E ; 58 FMs, strobe1; 58 FMs, strobe 2). Each signal is digitized into 2 bytes. Thus, each event represents 352 bytes. Each PM pulse is digitized at the maximum and in the middle part of the front. This give the background value of 1.5%.

Recording takes place in the "event-by-event" using a personal computer with Intel Xeon processor at event rates 15 events/s. Reading time of one event is 35 μs . Dead time introduced by DAQ is 41 μs . Throughput - 10 MB/s. In this Project, we plan move to a VME standard our trigger system (which is currently implemented via 15 years old CAMAC blocks) which has a higher degree of integration. Constructions made in the VME standard are more compact and more reliable.

Figure 9 shows the typical two-dimensional spectrum (dE - E) of the telescopes where clearly visible areas corresponding fragment registration from helium to magnesium. Thirty telescopes allow spectroscopic measurement and correlation measurement in respect to relative angles (from 10° to 180°) or relative velocities.

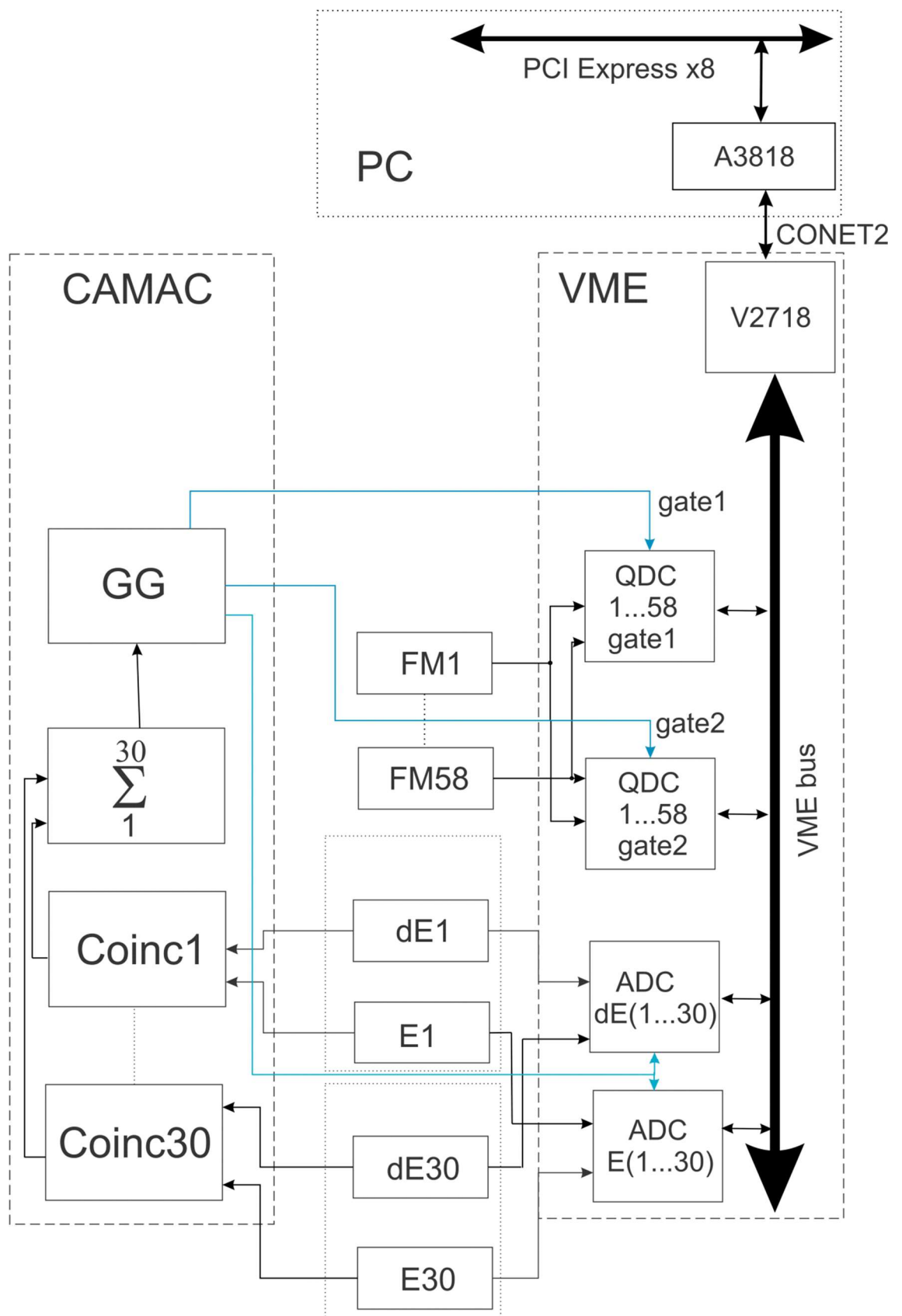


Fig. 8. Schematic view of data collection:
ADC – multievent analog to digital conversion channels, *QDC* – multievent charge to digital conversion channels, *V2718* – VME-PCI optical link bridge, *A3818* – PCI express optical link.

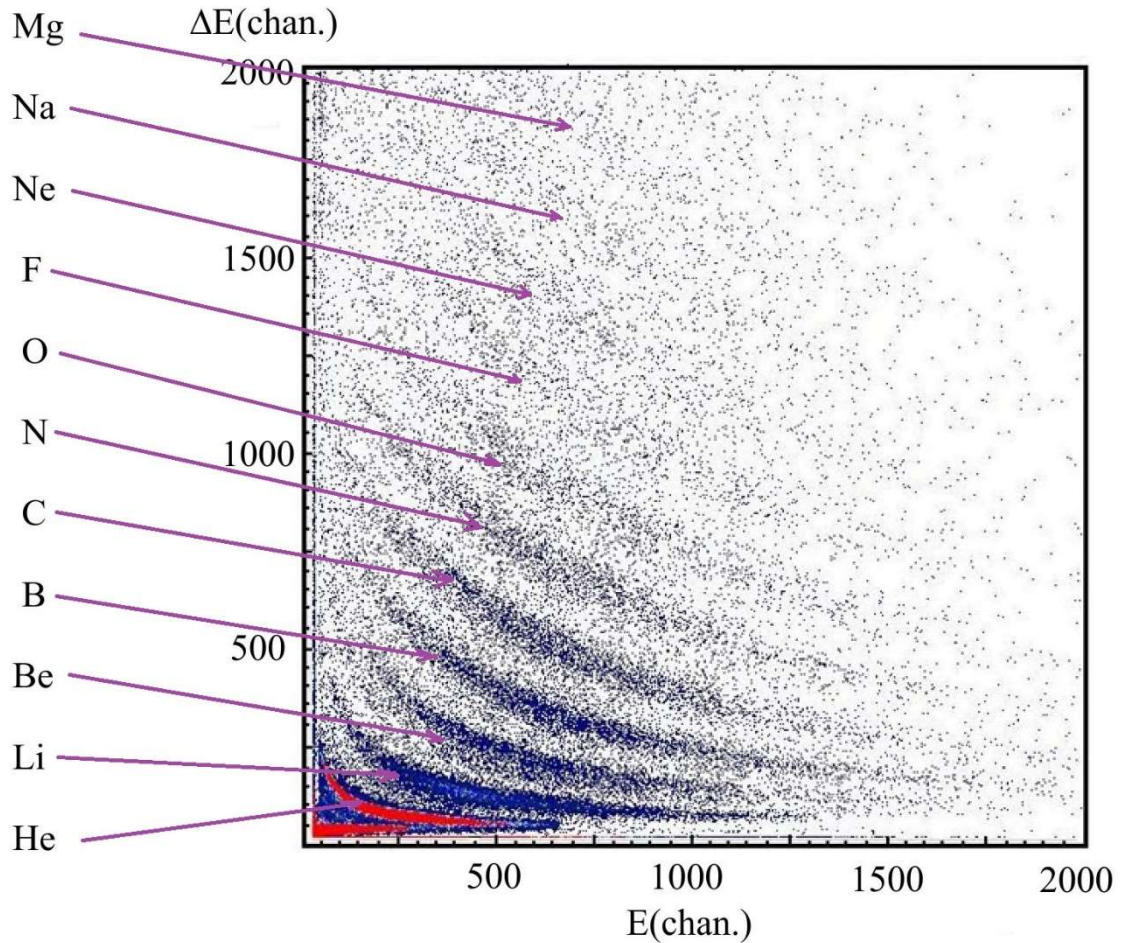


Fig. 9. Two-dimensional spectrum of fragments produced in $d(4.4 \text{ GeV}) + \text{Au}$ reaction.

THE MAIN EXPERIMENTAL RESULTS.

1. First proved experimentally that for hot nuclei (with an excitation energy of more than 3 MeV per nucleon) produced by relativistic light ion beams (protons, deuterons, α -particles), evaporation of particles is replaced by a process of thermal nuclear multifragmentation. This – new type of decay of excited nuclei when occurs multiple emission of intermediate mass fragments. They – heavier than α -particles, but lighter fission fragments ($2 < Z < 20$) [11].
2. This process of “explosive” type occurring during time 10^{-22}s (40 fm/c). So short time is measured for the first time in the FASA group via fragments correlation analysis in respect to relative angles [12].
3. For the first time experimentally shown that multibody decay of hot nuclei occurs after their expansion due to the thermal pressure. It was found that the process of thermal multifragmentation has two characteristic volumes. The first volume $V_i \approx 3V_0$ corresponds to the time of fragments formation. This configuration is similar to “saddle” point of fission. The second characteristic configuration is similar to the breakup point in the normal fission. It corresponds to the volume $V_f \approx (5.0 \pm 0.5)V_0$ filled with separated fragments [13, 14].

4. The typical process temperature (4 – 6 MeV) is considerably less than the critical temperature T_c for the phase transition “liquid-gas”. The value of T_c is defined by the analyzing of charge distribution of fragments generated in p(8.1 GeV) + Au collisions: $T_c = (17 \pm 2)$ MeV [15]. Note that for many years was a dramatic difference between this value and that obtained by L. Moretto (LBL, Berkeley, USA) [16]. Recently, this contradiction was resolved in favor of our values [17].
5. Our works have shown for the first time radial flow in the hot nuclei due to the thermal pressure. The analysis of the collective energy of fragments with their charge gives an unexpected and interesting information about the spatial configuration of the system at the time of the breakup. Proved that the heavier fragments are produced closer to the center of the system due to the inhomogeneous density distribution in a highly excited nucleus [18].
6. In case of relativistic light ions and gold target there is at least “kinetic equilibrium” of the system is achieved before fragmentation take place is found in the results of rapidity analyses [19].
7. Time scale of the thermal multifragmentation in ${}^4\text{He}(4 \text{ GeV}) + \text{Au}$ collisions was measured in 2018 [20]. For the experimental determination of the time scale of the process, the IMF-IMF correlation function was analyzed in respect to the relative angle. The correlation function exhibits a minimum at relative angles of zero arising from Coulomb repulsion between the coincident fragments. The magnitude of this effect drastically depends on the mean emission time, since the longer the time separation of the fragments, the larger their space separation and the weaker the Coulomb repulsion. The time scale for IMF emission is estimated by comparison the measured correlation function (Fig. 10) to that obtained by the multi-body Coulomb trajectory calculations with τ as a parameter. In order to measure the IMF-IMF repulsion effect, the correlation function values at 26° was used. The quantity is shown in Fig. 11 as a function of mean life time of the system. The mean decay lifetime $\tau = 47 \pm 12$ fm/c, which corresponds to simultaneous multibody decay.

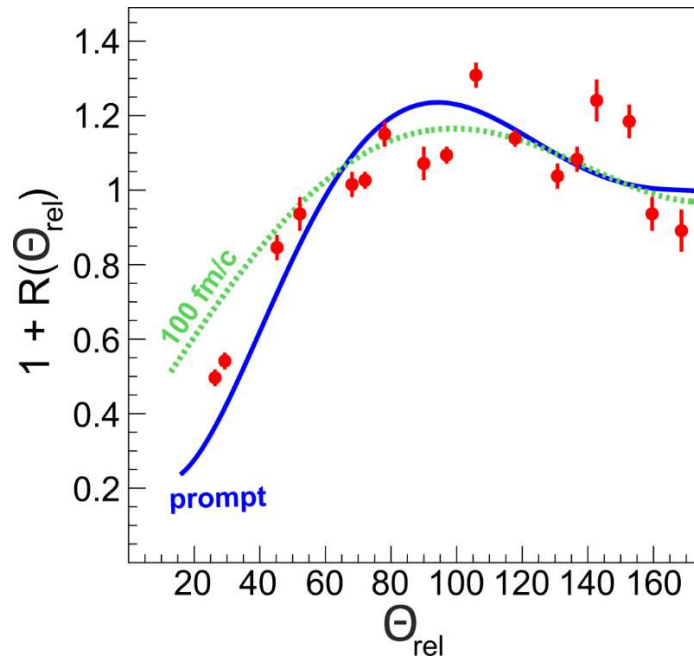


Fig. 10. Relative angle correlations functions for fragments ($2 < Z < 20$) produced in ${}^4\text{He}(4 \text{ GeV}) + \text{Au}$ reaction. Points – experimental data. Solid line – INC+SMM calculations with prompt secondary disintegration. Dotted line corresponds to INC+SMM calculations with mean time of secondary disintegration 100 fm/c.

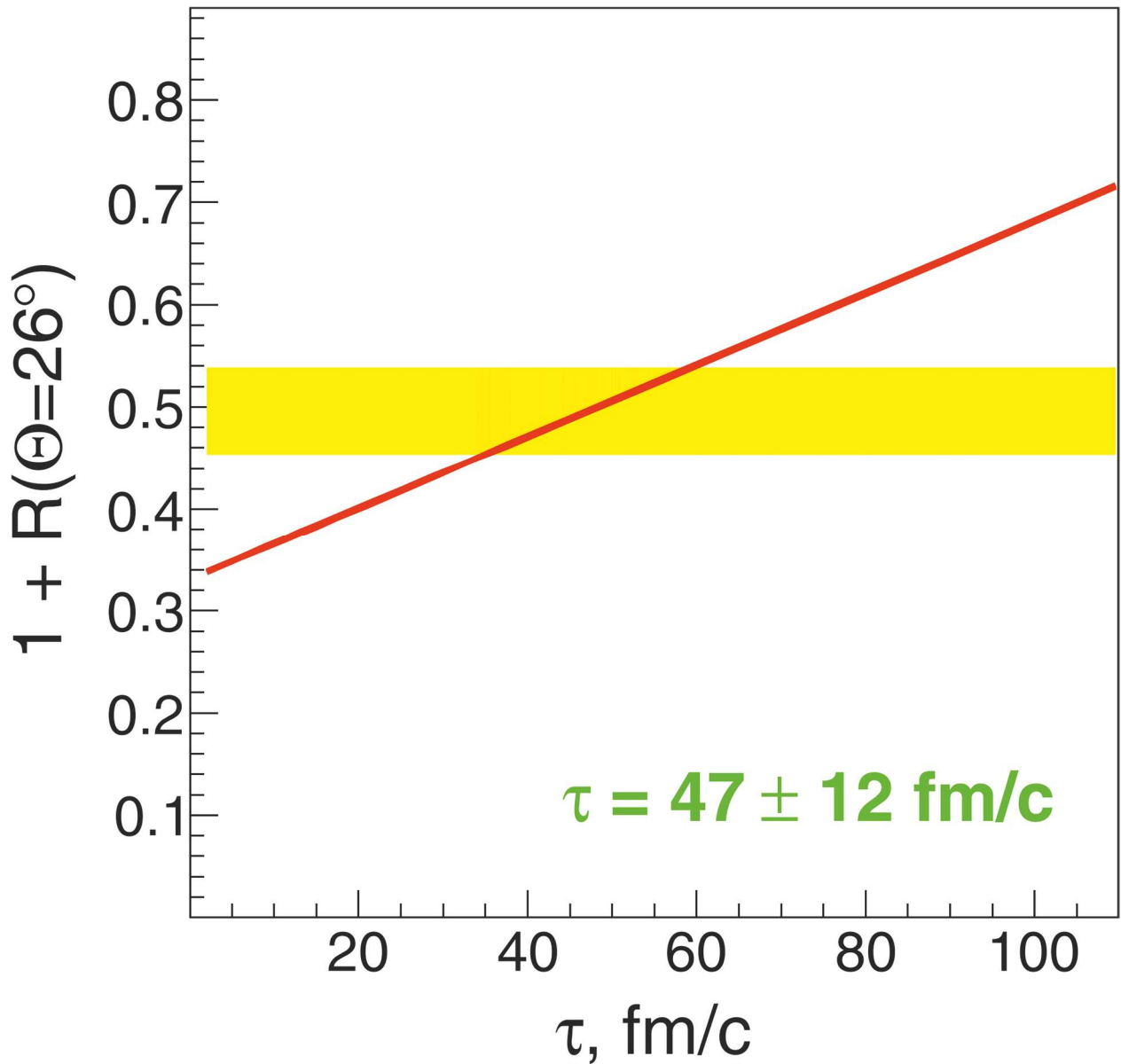


Fig. 11. Correlation function at relative angle 26° versus the mean decay time of the system. The experimental value is given by the horizontal band. The line is calculations (INC + SMM) using different decay time.

It is known that a very effective way to get hot nuclei are reactions produced by heavy ion beams [21-24]. However, this warming is accompanied by the excitation of collective degrees of freedom: nuclei are rotated, compressed, deformed. The study of these dynamic effects is interesting in itself. However, the collective effects make it difficult to obtain information on the thermodynamic properties of hot nuclear systems.

The picture is much easier when using relativistic beams of light particles. In this case, the collective degrees of freedom are weakly excited and excitation energy of nuclei is almost thermal. This gives grounds to tell about thermal multifragmentation in case of reactions of fast relativistic particles with heavy targets. The characteristics of this process are completely determined by the excitation energy. Light relativistic beams give a unique opportunity to study the thermodynamics of hot nuclear system. Note that detailed information about the process multifragmentation has important astrophysical applications [25], as the temperature on the surface of neutron stars is close to

temperature in multibody decay. Precise knowledge of the nuclei behavior with low density and temperature 5-10 MeV is essential for understanding the dynamics of supernova.

FASA collaboration successfully studied the “statistical” properties of hot nuclei, using Moscow-Copenhagen statistical model of multifragmentation in data analysis. This model has been significantly modified on base of our experimental data. A further object of the research is the *dynamics* of the process of multiple emission of fragments. In case of transition from proton beams to deuterons, α -particles, carbons, we observe a transition from a pure statistical process to processes in which dynamic effects begin to appear. We see that the fragments from target spectator have additional energy, which is provided by the collective flow. Therefore, the **objectives of the Project:**

1. Radial flow measurement as a function of the fragment charge;
 - a) Experimental measurement of kinetic energy spectra.
 - b) Calculation of the fragments kinetic energy spectra using a cascade and statistical models (with flow and without flow).
 - c) Comparison of empirical and theoretical distributions via Pirson criterion.
2. Measuring the velocity of the source and understanding the degree of equilibration involved in the disassembly process;
 - a) Analysis of the invariant cross sections as a function of the longitudinal and transverse velocity of the fragment.
 - b) The algorithm for obtaining the source velocity with errors is described in detail in the work [19].
3. New measurements of the correlation function with respect to the relative angles of the intermediate-mass fragments for the collisions of relativistic light ions with a gold target.
 - a) Experimental correlation function calculation from relative angles.
 - b) Computation of correlation functions based on calculations using a cascade and statistical models with different system lifetime.
 - c) Obtaining the time scale of the process with errors according to the procedure described in the work [20].

The requested acceleration time (with a beam intensity of more than 10^9 particles per spill) will allow to perform the tasks of the Project with an accuracy of several percent.

EXPECTED RESULTS.

- 1) Measuring the magnitude of the radial flow as a function of the fragment charge will give information about the distribution of fragments in the freeze-out volume.
- 2) Analysis of the invariant cross sections as a function of the longitudinal and transverse velocity of the fragment will allow us to determine degree of equilibration in a reaction, as well as determining the average source velocity.
- 3) Carrying out new measurements of the correlation function for the relative velocity (relative angles) intermediate-mass fragments ($2 < Z < 20$) for collisions of relativistic light ions with heavy targets. This will provide detailed information about the average time of system disintegration and about system configuration at the break-up time

The results will be sent to refereed journals for publication.
One, two publications per year.

PUBLICATIONS OF FASA GROUP FOR THE LAST THREE YEARS.

1. «Source velocity at relativistic beams of ^4He », Bulletin of the Russian Academy of Sciences. Physics (2016) Vol. 80, No. 3, 330;
2. «Study of the source velocity with the light relativistic ions at CBM», CBM Progress Report 2016 (2017) 187;
3. «Source velocity at relativistic beams of ^4He », J. Astrophys. Aerospace Technol. (2017) Vol. 5, No. 2, 48;
4. «Time scale of the thermal multifragmentation in $^4\text{He}(4\text{ GeV}) + \text{Au}$ collisions», Proceedings of the Academy of Sciences, physical series (2018) Vol. 82, No. 6, 711;
5. «Time scale of the thermal multifragmentation in $^4\text{He} + \text{Au}$ at FAIR energies», CBM Progress Report 2017 (2018) 162;
6. «Radial flow in the interaction of relativistic deuterons with a gold target», LXVIII International conference “NUCLEUS 2018”, book of abstracts, July 2-6 (2018) Voronezh, 73.

The results of the work were reported at conferences:

1. International conference **NUCLEUS-2017**.
September 12-15, 2017, Almaty, Republic of Kazakhstan;
2. 2nd International Conference on Atomic and Nuclear Physics.
November 08-09, 2017 at Las Vegas, USA;
3. LXVIII International conference **NUCLEUS-2018**.
July 2-6, 2018, Voronezh, Russia.
4. 4th International conference on Atomic and Nuclear Physics.
October 26-27, 2018, Boston, USA.

This work has the support by the Russian Foundation for Basic Research, project № 19-02-00499.

TIME SCALE OF THE PROJECT

1. Update trigger system FASA device from CAMAC to faster VME system: 2019-2021;
2. Experiments with the FASA device on the Nuclotron beams of relativistic light ions:
2020 – experiments using alpha beam;
50 hours: 4 GeV energy, intensity more than 10^9 particles per spill;
50 hours: 10 GeV energy, intensity more than 10^9 particles per spill;
50 hours: 16 GeV energy, intensity more than 10^9 particles per spill;
2021 – experiments using carbon beam;
50 hours: 10 GeV energy, intensity more than 10^9 particles per spill;
50 hours: 30 GeV energy, intensity more than 10^9 particles per spill;
50 hours: 48 GeV energy, intensity more than 10^9 particles per spill;
50 hours of acceleration time with the specified intensity will allow to register a million events, the analysis of which allow to determine the measured values with percentage accuracy.
3. Analysis of the experimental data using both statistical and dynamic models: 2019-2021;

4. Publication of the results in the form of articles in refereed journals (one or two publications a year): 2019-2021;

There are no risks in the implementation of the Project, as there is a working device and working people.

REFERENCES.

1. R. Wada, et al., Phys. Rev. C 99, 024616 (2019)
2. W. Lin, et al., Phys. Rev. C 97, 054615 (2018)
3. J. Brzychczyk, et al., Phys. Rev. C 98, 054606 (2018)
4. V.D. Toneev, et al., Nucl. Phys. A 519, 463 (1990)
5. W.A. Friedman, Phys. Rev. C 42, 667 (1990).
6. J.P. Bondorf, et al., Phys. Rept. 257, 133 (1995)
7. V.V. Kirakosyan, et al., Instr. And Exp. Techniques. Vol. 51, No. 2, 159 (2008)
8. S.P. Avdeyev, et al., Nucl. Instrum. Methods A 332, 149 (1993)
9. Yu.T. Vydai, Yu.A. Tsirlin, and E.F. Chaikovskii, Izv. Akad. Nauk SSSR, Ser. Fiz., 38, 1374 (1974)
10. A. Quinton, et al., Phys. Rev., 115, 886 (1959)
11. V. Lips, et al., Phys. Rev. Lett. 72, 1604 (1994)
12. V. Lips, et al., Phys. Lett. B 338, 141 (1994)
13. V.A. Karnaukhov, et al., Phys. Rev. C 70, 041601 (2004)
14. V.A. Karnaukhov, et al., Nucl. Phys. A 749, 65c (2005)
15. V.A. Karnaukhov, et al., Nucl. Phys. A 734, 520 (2004)
16. J.B. Elloitt, et al., Phys. Rev. Lett. 88, 042701 (2002)
17. V.A. Karnaukhov, et al., J. Phys. G: Nucl. Part. Phys. 40, 058001 (2pp) (2013)
18. S.P. Avdeyev, et al., Phys. Lett. B 503, 256 (2001)
19. S.P. Avdeyev, et al., Bulletin of the Russian Academy of Sciences. Phys., Vol. 80, No. 3, 330 (2016)
20. S.P. Avdeyev et al., Bulletin of the RAS, Phys., 82, No. 6, 711 (2018)
21. N. Buyukcizmeci et al., J. Phys. G: Nucl. Part. Phys. 39, 115102 (10pp) (2012)
22. M. Fidelus et al., Phys. Rev. C 89, 054617 (2014)
23. H. Imal et al., Phys. Rev. C 91, 034605 (2015)
24. S. Barlini et al., Phys. Rev. C 87, 054607 (2013)
25. A.S. Botvina and I.N. Mishustin, Nucl. Phys. A 843, 98 (2010)

Percentage of the time that authors will spend on a Project.

| | |
|-------------------|------|
| S.P. Avdeyev | 100% |
| H.Yu. Abramyan | 30% |
| A.S. Botvina | 30% |
| W. Karcz | 100% |
| V.V. Kirakosyan | 50% |
| L.V. Karnushina | 70% |
| E.M. Kozulin | 50% |
| A.G. Litvinenko | 30% |
| E. Norbeck | 30% |
| V.F. Peresedov | 30% |
| P.A. Rukoyatkin | 30% |
| V.I. Stegaylov | 50% |
| O.V. Strekalovsky | 30% |

Schedule proposal and resources required for the implementation of the Project

FASA
(Project title)

| Expenditures, resources, financing sources | | Costs (k\$) Resource requirements | Proposals of the Laboratory on the distribution of finances and resources | | | | |
|--|---------------------------------|---|---|----------------------|----------------------|----------------------|--|
| | | | 1 st year | 2 nd year | 3 rd year | 4 th year | |
| Expenditures | VME blocks | 30 | 10 | 10 | 10 | | |
| | Construction/repair of premises | - | - | - | - | | |
| | s/b detectors | 6 | 2 | 2 | 2 | | |
| Required resource | Standard hour | Nuclotron accelerator | 300 hours | 0 | 150 | 150 | |
| Financing sources | Budgetary resources | Budget expenditures including foreign-currency resources. | 36 | 12 | 12 | 12 | |
| | External resources | RFBR grant | 45 | 15 | 15 | 15 | |

PROJECT LEADER



Estimated expenditures for the Project PROPERTIES OF HOT NUCLEI ON RELATIVISTIC BEAMS OF THE NUCLOTRON/NICA COMPLEX

(full title of Project)

| Expenditure items | Full cost | 1 st year | 2 nd year | 3 rd year... |
|---------------------------------|-----------|----------------------|----------------------|-------------------------|
| Direct expenses for the Project | | | | |
| 1. Accelerator Nuclotron | 300 hours | 0 | 150 | 150 |
| 2. VME blocks | 30 k\$ | 10 | 10 | 10 |
| 3. s/b detectors | 6 k\$ | 2 | 2 | 2 |
| 4. Travel allowance, including: | 42 k\$ | 14 | 14 | 14 |
| a) non-rouble zone countries | 36 | 12 | 12 | 12 |
| b) rouble zone countries | 6 | 2 | 2 | 2 |
| c) protocol-based | | | | |
| Total direct expenses | 78 k\$ | 26 k\$ | 26 k\$ | 26 k\$ |

PROJECT LEADER

LABORATORY DIRECTOR

LABORATORY CHIEF ENGINEER-ECONOMIST